Solar Phys (2019) 294:9
https://doi.org/10.1007/s11207-019-1400-3

Characteristics of SEP Events and Their Solar Origin During the Evolution of Active Region NOAA 10069

L.K. Kashapova[1] · R. Miteva[2] · I.N. Myagkova[3] · A.V. Bogomolov[3]

Received: 5 February 2018 / Accepted: 11 January 2019

Abstract We present the results of a comparative analysis of the properties of a series of successive solar flares, which occurred in active region (AR) 10069 in August 2002, and the associated solar energetic particle (SEP) events. The active region was extremely flare productive during its evolution. The solar flare characteristics are based on X-ray and radio emission data: maximum detected photon energies and spectral index, delays between microwave, metric-radio and, hard X-ray emissions. The coronal mass ejections (CMEs) are characterized by their projected speed. The SEP properties are described by the relative electron to proton abundance as well as by the abundance of lower relative to higher energy particles. The analysis carried out supports some previous results obtained by large statistical studies, but at the same time refutes others. For example, the set of analyzed events that occurred in the AR did not show clear evidence of the big flare syndrome though the large proton events observed near Earth were always accompanied by CMEs. Some of the peculiar observations could be the result of the magnetic topology of the AR.

Keywords Solar energetic particles · Coronal mass ejections · Flares · X-ray emission · Microwaves and radio emission

✉ L.K. Kashapova
lkk@iszf.irk.ru

R. Miteva
rmiteva@space.bas.bg

I.N. Myagkova
irina@srd.sinp.msu.ru

A.V. Bogomolov
aabboogg@sinp.msu.ru

1 Institute of Solar-Terrestrial Physics, SB Russian Academy of Sciences, 664033 Irkutsk, Russia

2 Space Research and Technology Institute, Bulgarian Academy of Sciences, 1113 Sofia, Bulgaria

3 Skobeltsyn Institute of Nuclear Physics, Moscow State University, 119991 Moscow, Russia

Published online: 22 January 2019

1. Introduction

Transient enhancements of electron, proton, and ion fluxes in interplanetary (IP) space called solar energetic particle (SEP) events, also named solar cosmic rays, together with their solar sources are a topic of ongoing research (*e.g.* Reames, 1999, 2015; Gopalswamy *et al.*, 2008; Desai and Giacalone, 2016). Two particle accelerators of solar origin are usually considered, namely reconnection processes during flares (see, *e.g.*, Cane, Erickson, and Prestage, 2002) and shock acceleration driven by coronal mass ejections (CMEs) (Reames, 1999, 2015). Apart from *in situ* observations and numerical modeling of particle fluxes, electromagnetic (EM) emission signatures (mostly from electrons) are used as diagnostics of the physical processes that take place from Sun to Earth.

Nowadays we have two respective trackers of the acceleration processes during solar flares – hard X-ray (HXR) emission and microwave (MW) non-thermal gyrosynchrotron emission. Both types of emission are produced by accelerated non-thermal electrons (see, *e.g.*, Lin, 2011). The assumption is that the low cut-off energy of non-thermal electrons producing hard X-ray emission is about 20 keV. The high-temperature thermal emission could shift this cut-off to energies above 30 keV. However, time profiles of HXR emission in energy bands corresponding to the non-thermal emission are used as the markers of the acceleration process in solar flares (Lin, 2011; Fletcher *et al.*, 2011). Moreover, the photon or electron spectral index could be an indication of the height where the acceleration occurs. The collisional thick target model predicts deeper penetration of more energetic electrons into the solar atmosphere. As a result, the HXR emission can be detected from the lower levels of the legs of a flare loop and with harder power-law spectra. This assumption is used for explaining the spectral index hardening during solar flares (see, *e.g.*, O'Flannagain *et al.*, 2013).

The HXR emission is a bremsstrahlung emission of accelerated electrons going downwards to lower and denser layers of the solar atmosphere. The accelerated electrons propagating from the primary energy release location could also get into upper and less dense layers of the solar atmosphere. There the conditions are favorable for generating the non-thermal gyrosynchrotron emission (Dulk, 1985). If the electrons emitting in HXR and microwaves are from the same population, then their time profiles should match. Any delays or disagreements between the profiles could be an indicator of peculiarity in flare loop topology or energy release scenario (see, for example, Bastian, Benz, and Gary, 1998; White *et al.*, 2011).

The microwave emission of solar flares above 2 GHz is usually incoherent gyrosynchrotron emission of mildly and highly relativistic electrons (see Dulk, 1985). The radio emission below 2 GHz is usually generated by coherent emission mechanisms and characterizes the various sets of burst classifications using the dynamic spectra (see Bastian, Benz, and Gary, 1998). The nature of these bursts could be different – from shock waves of type II bursts to propagating or trapped accelerated electrons (type III and IV bursts, respectively). The comparative analysis of HXR and radio coherent emission allows understanding the scenario of solar accelerated electron beams propagation in the IP space (see, *e.g.*, White *et al.*, 2011; Reid and Ratcliffe, 2014).

The study of particle acceleration near the Sun, their transport through IP space, and possible space weather effects are essential to provide reliable forecasts. An important aspect is the solar origin of the particles (solar flares or CMEs), since forecasting can be based on remote observations of flare and CME signatures and modeling of the underlying acceleration processes.

A common approach to identifying the SEP origin is selecting the strongest flare and fastest CME in a time interval prior to the SEP increase at 1 AU. This relates SEP events

of different intensity levels to flares and CMEs. Such analyses are further expanded into statistical studies, by calculating Pearson correlation coefficients between the peak SEP flux on the one hand and the flare and CME parameters on the other hand. The correlation coefficients are used to indicate whether, on average, the flare or CME plays a more important role in the particle acceleration. Various selection criteria on the SEP sample, however, led to contradictory results which fueled the debate on the SEP origin. Overall, the more numerous the SEP sample, the more difficult it is to identify a dominant flare *vs.* CME contribution to the particle acceleration when using correlations (Cane, Richardson, and von Rosenvinge, 2010), since the results are the same within the statistical uncertainty (Miteva *et al.*, 2013a). A study by Dierckxsens *et al.* (2015) on the SEP energy dependence indicated statistically different correlations only for the ≤ 10 MeV proton fluxes (with CMEs) and ≥ 100 MeV proton fluxes (with flares, respectively). However, this method did not show clear tendencies for the intermediate energy range of the protons. Linear correlation coefficients are usually calculated between a selected pair of parameters, namely between the proton intensity (or fluence), on one side, and a parameter characterizing the solar origin, on the other side. For the latter, either the flare class or fluence or the linear CME speed or CME angular width are used. However, these are not independent from each other (Miteva *et al.*, 2013a; Salas-Matamoros and Klein, 2015) and the resulting correlations account for mixed solar origin influences. This limitation was relaxed by using partial correlation coefficients (Trottet *et al.*, 2015) that filtered out the interdependence on a third parameter. The results also revealed higher correlations while using flare fluence than GOES flare class.

The spectral properties of SEP events, *i.e.* element abundances (Reames, 2015) or the ratio of proton to electron flux (Daibog, Melnikov, and Stolpovskii, 1993), are often used to relate to the 'impulsive' or 'gradual' scenario of the SEP origin. Studies using flare microwave bursts and relative abundance of energetic electrons and protons (so-called 'e/p ratio') revealed that a higher e/p ratio corresponds to impulsive flare bursts (Daibog *et al.*, 1989). However, in a later study Daibog, Melnikov, and Stolpovskii (1993) found weak impulsive flares associated with proton-rich events. This led the authors to conclude that the possibility for protons to escape is as important as the efficiency of acceleration. The suggested explanation was that the dynamics of particles in flare loops is strongly influenced by the efficiency to escape into interplanetary space. The authors proposed that weak impulsive events take place in large size flare loops stretched high into the corona where the magnetic field in the flare loop is weak and the level of excited turbulence is rather low. This could result into weak diffusion of protons into the loss cone, long lifetime of particles in the loop, and a relatively high efficiency of their escape into the IP medium.

A different approach used to infer the SEP characteristics is based on the associated radio emission. Based on statistics over Solar Cycle (SC) 23 by Miteva *et al.* (2013b) and the extension into SC24 by Miteva, Samwel, and Krupar (2017), we found that the association between proton events and type III radio bursts is the highest over type II and IV radio bursts. Similar results were presented by Papaioannou *et al.* (2016) based on an event sample from 1997 to 2013. Kouloumvakos *et al.* (2015) presented a comparative temporal study of derived SEP onset times and associated radio emissions. The authors found that in the majority of cases, the proton release is accompanied by both type III and II radio bursts. However, they also presented a good association rate for SEP events accompanied by type IIIs only, whereas type II bursts showed the worst association with SEP events. Nevertheless, it is difficult to establish a clear-cut distinction between flare-related and CME-related SEP events based on burst type as these can be produced by either accelerator.

Previous SEP studies did not usually take into account the peculiarity or properties of the active region (AR). A recent study by Thalmann *et al.* (2015) was devoted to an AR that

was unusually large and produced many X-class flares mostly not followed by CMEs. This means that the scenario of the flares produced by this AR was distinctive from the scenario of most two-ribbon flares. This peculiarity was connected to a magnetic arcade. Alternatively, the magnetic topology of such unusually productive region should not change significantly during the 'active' period of its evolution. One can expect such active region to produce SEP events with similar properties, which follow the development of their origin. Another recent study by Bronarska and Michalek (2017) investigates the statistical properties of ARs producing large SEP events. Based on the statistical analysis of 84 SEP events they showed that SEP events were more likely associated with ARs having complex magnetic structures. The other tendency was that ARs having a large and asymmetric penumbra were at the origin of the most energetic SEPs. The authors used McIntosh classification of ARs (McIntosh, 1990) in their analysis. We note that this classification reflects the evolution of ARs from onset to decay.

On the one hand, it means that the evolution of the magnetic topology of ARs and their SEP productivity are related. On the other hand, ARs with different magnetic topology could have different SEP productivity. It is not evident if one of these factors dominates and how the previous statistical results depend on these factors. An analysis of the evolution of both SEP events and flares originating from the same AR could give more insight. The magnetic topology of this active region should not dramatically change.

In the present analysis we focus on the productivity of solar events in AR 10069 during August 2002. We analyze the properties of a series of energetic particle enhancements and the solar events regarded as their origin with the aim to reveal tendencies in their relationship. We carry out a detailed case study of events originating from AR 10069 and focus on the following issues:

- Are the most powerful flares producing the largest SEP events (big flare syndrome, Kahler, 1982) during the evolution of the active region under study?
- Is the high level of *in situ* protons always associated with CMEs?
- Softening or hardening of the HXR spectral index during the flare can indicate the acceleration site is moving up or down in the solar atmosphere (O'Flannagain *et al.*, 2013). In case of the evolution of the spectral index from flare to flare within the same active region, it also can indicate a relatively higher or lower location of the acceleration. The increase of the acceleration height is most likely a result of the rising of the active region loops due to the emerging magnetic flux. Do changes of the spectral index indicate the role of the emerging magnetic flux in the SEP-flare production?
- Under the assumption that gyrosynchrotron microwave emission indicates particle acceleration in the low atmosphere and that the meter radio emission is indicative of the subsequent propagation of the accelerated electrons through the solar corona, the delay between these two wavelength ranges is used as diagnostic of any temporal peculiarities of the acceleration and propagation of the energetic particles. Are there some tendencies of flares followed or not by SEP events?

2. Observations and Data Analysis

For our analysis we selected observations of *in situ* protons and electrons, flare emission in HXRs, metric-radio (MHz frequencies), and cm-radio or microwaves (GHz frequencies), and the data from CMEs that occurred from 17 to 24 August 2002 during the evolution of AR 10069.

Information about the proton fluxes of the SEP events is taken from GOES-10 spacecraft. The satellite is in geostationary orbit with an altitude of about 36 000 km, an inclination of about 0°, and a longitude of 135°W (Onsager *et al.*, 1996). GOES-10 satellite provides the proton fluxes in seven energy bands: 0.6 – 4, 4 – 9, 9 – 15, 15 – 44, 40 – 80, 80 – 165, 165 – 500 MeV measured by the *Energetic Particles Sensor* (EPS) instrument.[1] We use here two of the channels and recalculate the data into integral values, namely proton flux > 10 MeV (F_{p10}) and > 30 MeV (F_{p30}) with a 1-h time resolution. The electron fluxes with energies 53 – 103 (F_{e53}) and 175 – 315 keV (F_{e175}) were measured by the *Electron, Proton, and Alpha Monitor* (EPAM) onboard the *Advanced Composition Explorer* (ACE) spacecraft (1-h data),[2] located in the libration point L1 at about 1.5 million km from Earth towards the Sun (Stone *et al.*, 1998).

For the flare HXR emission we used data from the *Solar Neutrons and Gamma-rays* (SONG) instrument[3] installed onboard CORONAS-F (Kuznetsov *et al.*, 2014), which measures HXR and gamma-ray emission in a wide energy range, *i.e.* 0.03 – 200 MeV. Furthermore, HXR observations when the satellite passes the polar caps are only possible during SEP quiet times to avoid contamination by particle fluxes. In August 2002, the energy ranges for the first six energy channels corresponded to 36 – 72, 72 – 180, 180 – 600 keV and 0.6 – 1.56, 1.56 – 4.8, and 4.8 – 8.4 MeV. We complemented the HXR data with measurements from the *Reuven Ramaty High-Energy Solar Spectroscopic Imager* (RHESSI: Lin *et al.*, 2002).

Information on the flare class is taken from the GOES flare catalog.[4] We used the time of the CME first appearance in the *Large Angle and Spectroscopic Coronagraph* (LASCO) C2 onboard the *Solar and Heliospheric Observatory* (SOHO), the results of the extrapolation of the CME onset and other additional information from the NASA CME catalog[5] for checking the relation between the studied flares and CMEs. The values of the projected linear CME speed from this catalog were used in the analysis.

We base our selection criteria on HXR emission as this is the most reliable characteristic of particle acceleration during solar flares. Furthermore, we require data with few instrumental effects, especially attenuator changes. That is why we used the HXR time profiles provided by the SONG instrument. The flare event list is adopted from Bogomolov *et al.* (2014). We decided to used RHESSI data to improve the statistics. The solar flare should occur in the same active region with a HXR flux with energy above 50 keV and without attenuator changes. One additional case (22 August 2002) satisfied these criteria. Photon flux enhancements with energies above 70 keV were detected following nine flares in the considered time interval (Bogomolov *et al.*, 2014) and gamma rays with energies above 600 keV were detected in five flares (Myagkova *et al.*, 2007).

Figure 1 shows the time profiles of proton and electron fluxes during the selected eight day time period. We associated the SEP event with the flare and CME that preceded the particle event. The obtained results agree with the solar origin reported in the Catalog of Solar Proton Events in the 23rd Cycle of Solar Activity (1996 – 2008) edited by Logachev.[6] The onset times of the flares that took place in AR 10069 are marked by vertical lines. We

[1] https://satdat.ngdc.noaa.gov/sem/goes/data/new_avg/2002/08/goes10/csv/.

[2] https://cdaweb.sci.gsfc.nasa.gov/index.html.

[3] We used the SONG data via private communication and with permission of the authors of the experiment on the CORONAS-F satellite as the data are not publicly accessible.

[4] https://hesperia.gsfc.nasa.gov/goes/goes_event_listings/.

[5] https://cdaw.gsfc.nasa.gov/CME_list/.

[6] http://www.wdcb.ru/stp/data/SPE/.

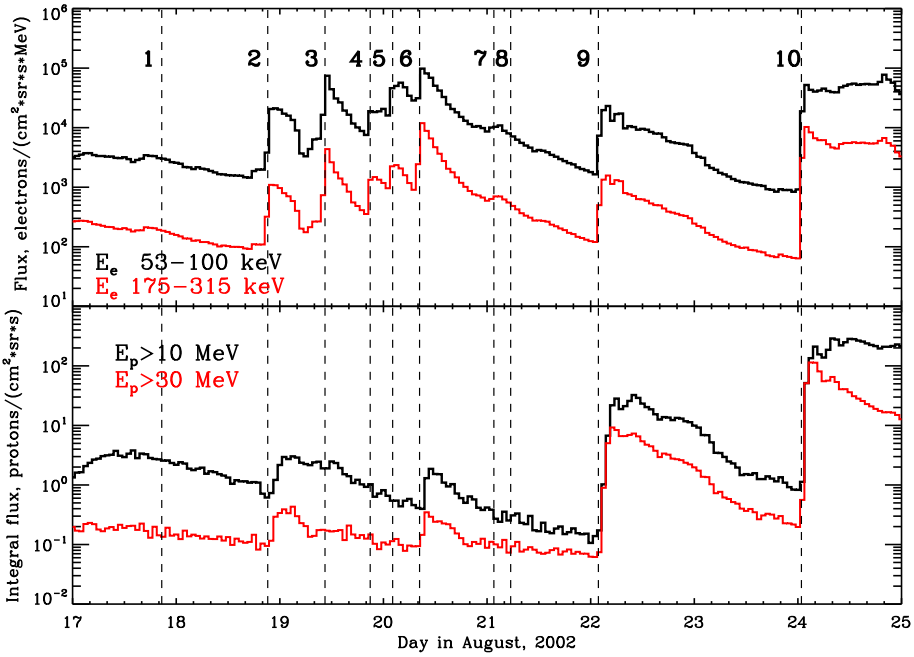

Figure 1 Evolution of electron (*upper plot*) and proton fluxes (*lower plot*) in the period 17 to 25 August 2005, see Table 1. *Vertical lines* show the onset times of the solar flares under consideration.

note that nine out of ten flares are followed by electron enhancements to be compared to only five individual proton events observed in the same time period. We used the lowest (53 – 103 keV) and highest (175 – 315 keV) energy ranges of the ACE/EPAM instrument in order to calculate the spectral index of the electrons in the SEPs. Due to the small flux amplitude for most of the proton events, we selected the two lowest energy channels, > 10 and > 30 MeV. The pre-event particle flux value is subtracted from the maximum value for the flux for each proton and electron event and referred to as peak flux. The results are summarized in Table 1. The electron (proton) flux ratio between the lowest and the highest energy channel, denoted by R_{E} (R_{P}, respectively), and the electron-to-proton flux ratio of electrons with 175 – 313 keV energies to protons with energies above 30 MeV, denoted by $F_{\mathrm{e}}/F_{\mathrm{p}}$, are also calculated.

The parameters of the SEP-associated flares and CMEs are also shown in Table 1: GOES flare class, time of flare onset, flare location, maximum energy channel in which HXRs and/or gamma-rays were detected, spectral index γ, CME projected speed, radio emission type, and two temporal delays, respectively. We followed Bogomolov *et al.* (2014) for the analysis of flare HXR and MW emission. The HXR photon spectral index γ is obtained under assumption of a power-law distribution for the non-thermal part of the X-ray spectrum. The photon spectral index for most flares in Table 1 was estimated from the response in channels 36 – 72, 72 – 180, and 180 – 600 keV. Since no signal was observed in the high-energy channels for the M2.2 flare on 18 August 2002 and the C5.5 flare on 20 August 2002, the reported spectral indices are calculated from the ratio of the first two channels.

Microwave (at 15.4 GHz) and metric-radio data (in the MHz range) covering the full period of eight days analyzed in our study was available from the *Radio Solar Telescope Network* (RSTN), a ground-based network of nearly identical stations. All radio stations provide

Table 1 Parameters of the SEP events and the SEP-related flares, CMEs, and radio emission signatures. The abbreviations correspond to R_E: electron flux ratio F_{e53} to F_{e175}, R_P: proton flux ratio F_{p10} to F_{p30}, $Delay_1$: 245 MHz–HXR, $Delay_2$: 40 MHz–HXR. For further abbreviations and explanations see text.

No.	Event date dd-mon-yyyy	F_{p30} $(cm^2\,s\,sr)^{-1}$	F_{e175} $(cm^2\,s\,sr)^{-1}$	R_P	R_E	F_e/F_p	Flare GOES class	Flare onset (UT)	Flare location	Max energy band (MeV)	γ	CME speed $(km\,s^{-1})$	Radio burst type	$Delay_1$/ $Delay_2$ (s)	Delay HXR–MW (s)
1	17-Aug-2002	no	no	–	–	–	M3.4	20:39	S06W05	0.18 – 0.6	3.7	–	no radio	no radio	15
2	18-Aug-2002	0.4	133	8.8	6.5	332.5	M2.2	21:12	S12W19	0.07 – 0.18	2.7	682	II, III	10/10	20
3	19-Aug-2002	0.1	588	22.5	5.7	5880	M2.0	10:28	S12W25	0.18 – 0.6	3.6	549	III	0/−18	0
4	19-Aug-2002	no	161	–	3.8	–	M3.1	20:56	S11W33	0.18 – 0.6	3.8	–	III	4/5	3
5	20-Aug-2002	no	168	–	11.2	–	C5.5	02:08	S10W35	0.07 – 0.18	3.2	–	III	83/17	0
6	20-Aug-2002	0.5	1549	5	2.1	3080	M3.4	08:22	S10W38	4.8 – 8.4	2.1	1099	III	7/23	1
7	21-Aug-2002	no	28	–	25.2	–	M1.4	01:35	S11W47	0.6 – 1.56	2.6	–	III	0/20	0
8	21-Aug-2002	no	no	–	–	–	X1.0	05:28	S12W51	4.8 – 8.4	2.9	268	II, III	0/30	0
9	22-Aug-2002	11	166	2.1	5.1	15.1	M5.4	01:47	S07W51	0.1 – 0.3	3.4	998	II, III	90/18	0
10	24-Aug-2002	100	1386	1.5	1.7	13.9	X3.1	00:49	S02W81	4.8 – 8.4	3.0	1913	II, III	70/500	0

radio flux observations at eight discrete frequencies between 245 MHz and 15.4 GHz (for the instrument description see, *e.g.*, Kennewell and Cornelius, 1983) and, in addition, also spectral observations from 25 MHz to 180 MHz. Thus information at lower frequencies is extracted from the RSTN dynamic radio spectra, *e.g.* at the discrete frequencies of 40 and 150 MHz.

Furthermore, we identified radio emission signatures, namely radio burst types II and/or III (Table 1), and the results agree with previous studies (Cane, Richardson, and von Rosenvinge, 2010; Miteva *et al.*, 2013b). In the final two columns we added a quantitative estimation on the delay of the radio (245 MHz and 40 MHz, Delay_1) and MW emissions with respect to the HXR emission (Delay_2). The time difference was evaluated based on the peak time of the emissions. The time profiles of these emissions during the events in this study are shown in Figure 2.

3. Results

3.1. Event Description

Below we summarize each event in our study, describing the SEPs, the associated flares, CMEs, and radio emission signatures.

3.1.1. Event 1: 17 August 2002

An M3.4 flare event started at 20:39 UT without any related CME. We cannot clearly identify any new injection of particles into the IP medium on this day due to the ongoing particle event that started on 16 August 2002. In spite of significant emission in soft and hard X-rays, we found no response in the radio emission for the frequencies lower than 5 GHz. Due to the absence of type III bursts, we assume that the flare occurred in a magnetic configuration without open magnetic field lines. We also found a 15-s delay between the time profiles of MW emission at 15.4 GHz and the HXR emission. There could be two explanations for this delay. The accelerated electrons responsible for the HXR emission precipitate and produce the thermal electrons which fill up the flare loop and emit MW. Alternatively, the observed MW emission could be the result of a plasma mechanism in high-density flare loop.

3.1.2. Event 2: 18 August 2002

This event is associated with an M2.2 flare starting at 21:12 UT. The flare was followed by a CME with reported velocity of 682 $\text{km}\,\text{s}^{-1}$. Emission in MW and m-radio ranges is detected. In m-radio range this event is associated with both type II and type III bursts.

There is no delay between HXR and m-radio emissions (150 MHz) while the delays between HXRs with 40 and 245 MHz are both of 10 s, whereas with 15.4 GHz emission it is 20 s. An absence of delay for the 150 MHz emission could mean that this emission was generated closer to the primary energy release site than emissions in the other frequencies. The 10-s delays at lower and higher frequencies most probably reflect propagation effects. The hard photon spectral index of HXR emission (2.7) and the long delay between MW and HXR time profiles (20 s) indicate an absence of the conditions for direct MW emission of electrons or alternatively, the plasma is too dense. Particle events were observed in the 175 – 315 keV electron and > 30 MeV proton channels starting on 18 August and reached peak intensity the following day.

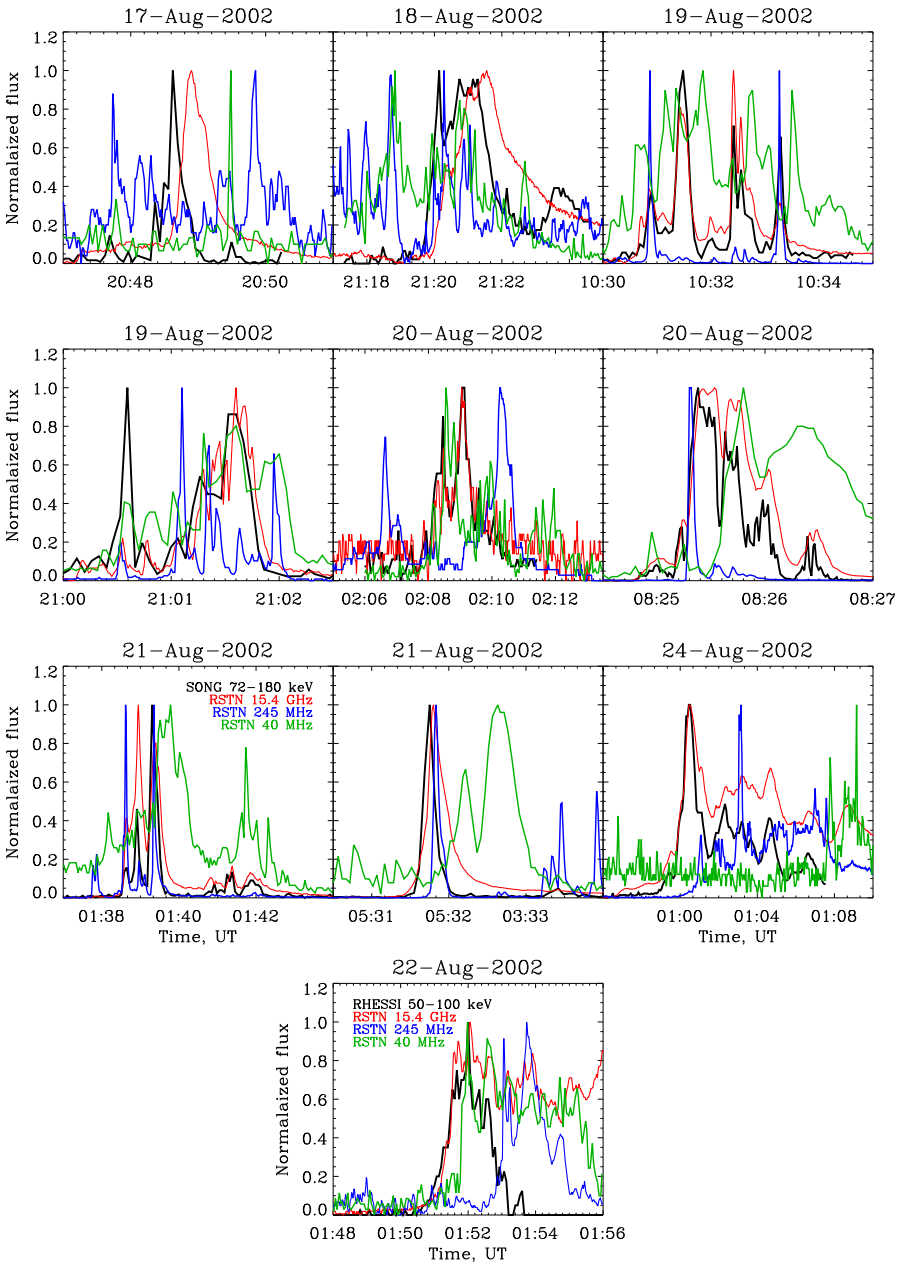

Figure 2 Comparison of the temporal profiles in HXR, radio, and MW spectral ranges for the considered events observed by SONG and RHESSI (for 22 August 2002).

3.1.3. Event 3: 19 August 2002 A

The M2.0 flare occurred at 10:28 UT and was associated with a CME (velocity is about 550 km s^{-1}). There is no evidence of type II bursts during this event. The absence of type IIs

could be explained by a low plasma density on the path of the shock wave propagation. The HXR photon spectral index γ is 3.6. The peculiarity of this event is the onset of radio emission at 150 MHz and 40 MHz earlier than HXR and MW emission. The combination of no delay between the HXR, and the emission up to 245 MHz with the soft spectral index of the HXR emission could be evidence of reconnection, *i.e.* the location of primary energy release, in the upper corona.

A new electron event is clearly seen to rise fast and peaks at about midday, whereas the proton event looks like the continued decay of the previous event. Here, we consider it as a true new injection but with very low intensity.

3.1.4. Event 4: 19 August 2002 B

The event is associated with the M3.1 flare that started at 20:56 UT with the HXR photon spectral index equal to 3.8. This event is accompanied by type III bursts. The radio emission taken at 150 MHz in this case has a delay with HXR emission of 3 s. The delay with 40 MHz is in good agreement with an average velocity of electrons in type IIIs, namely 0.3 times the speed of light (see, for example, Reid and Ratcliffe, 2014). A second electron injection at the end of this day can be observed, whereas no new proton event could be identified.

3.1.5. Event 5: 20 August 2002 A

During the associated GOES C5.5 flare (with an onset at 02:08 UT) X-ray emission above 20 – 30 keV was detected which is unusual for such weak flares. The m-radio range shows a presence of the type III bursts. There is no delay between the HXR and MW time profiles but there is a long delay between the HXRs and 245 MHz emission. Emission at this frequency is usually generating within the solar corona higher than MW emission but lower than 40 MHz emission. Such delay could correspond to the propagation of a CME-driven shock wave. However, there was no CME detected during this event. Another explanation could be that this emission is a result of filling the flare loops with heated plasma resulting from chromospheric evaporation (see description in Fletcher *et al.*, 2011). The delay between the 40 MHz emission and HXRs could be explained by the low velocity of electrons generating the type III bursts.

The electron event occurs at the beginning of the day, with no proton counterpart.

3.1.6. Event 6: 20 August 2002 B

The M3.4 flare occurred at 08:22 UT and was associated with a CME (with velocity close to 1100 $\mathrm{km\,s^{-1}}$). However, there is a detection of type III bursts only in the m-radio range. The absence of type II bursts could be explained by the low plasma density on the way of the shock wave propagation. This event has the hardest HXR photon spectral index in the sample (2.1). The delay between the MW and HXR time profiles is 1 s. These facts indicate low heights of primary energy release during this event. The delays relative to the HXR burst are increasing with decreasing frequency up to 245 MHz. The delay between the HXRs and 40 MHz bursts is 23 s.

Both proton and electron SEP events are identified.

3.1.7. Event 7: 21 August 2002 A

The M1.4 flare took place at 01:35 UT and was followed by a type III burst. There are no delays between the HXR bursts and 15.4 GHz and 245 MHz frequencies. The HXR photon

spectral index γ is 2.6. The delay at 40 MHz could be explained if we assume a slow electron velocity of the accompanying type IIIs.

A weak electron increase is noticed on the declining slope of Event 6. No new proton event is identified.

3.1.8. Event 8: 21 August 2002 B

The X1.0 flare started at 05:28 UT. It was followed by a slow CME (268 km s^{-1}) and type II and III bursts. The evolution of the HXR time profile coincided with the time profiles of the emission at 15.4 GHz and 245 MHz. The HXR photon index is 2.9. We obtained delays of about 24 – 30 s for the coherent emission (*i.e.* plasma emission signatures at m-radio range) only.

No particle event is observed.

3.1.9. Event 9: 22 August 2002

The M5.4 flare occurred at 01:47 UT accompanied by a fast CME with speed of 998 km s^{-1}. There are type II and III bursts observed in the m-radio range. The HXR photon spectral index γ is rather soft (3.4). There is no delay between HXR and MW time profiles but there are long delays between the HXRs and the burst at 245 MHz and 150 MHz frequencies of about 90 s for both. Such delays could be explained by the generation of a CME-driven shock wave. The delay at 40 MHz is 18 s and it is marginally within the type III electron speed range.

Strong electron and proton events are observed at the beginning of the day.

3.1.10. Event 10: 24 August 2002

The X3.1 flare started at 00:49 UT and was associated with a very fast CME, 1913 km s^{-1}. There are type II and type III bursts present in the m-radio range. The HXR photon spectral index γ is 3. There is no delay between HXR and MW time profiles but there are long delays with the bursts at m-radio frequencies. Such delays can only be explained by the generation of a CME shock wave. This is a probable case of energetic particle acceleration due to shock waves.

Strong electron and proton events are observed at the beginning of the day.

3.2. Dependencies

Various parameters are studied in order to find the presence or absence of a relationship between them. The widely used parameters characterizing solar flare are the GOES class (thermal emission of the flare), X-ray photon spectral index (emission of the accelerated electrons) and, indirectly, the velocity of the accompanying CME (Aschwanden *et al.*, 2017, or some equivalent of kinetic energy estimation). The SEP parameters could be described by the ratio of the electron (or proton) fluxes at different energy bands, equivalent to the electron (proton) spectral index, which mainly characterizes the abundance of high-energy particles (electrons or protons) for the given particle event. Additionally, the parameter used to characterize the relative abundance of the particle species is the electron-to-proton ratio.

Figure 3 shows scatter plots of the particle flux ratios at two energy bands, R_{E} for the electrons and R_{P} for the protons with respect to the CME projected speed, the GOES flare

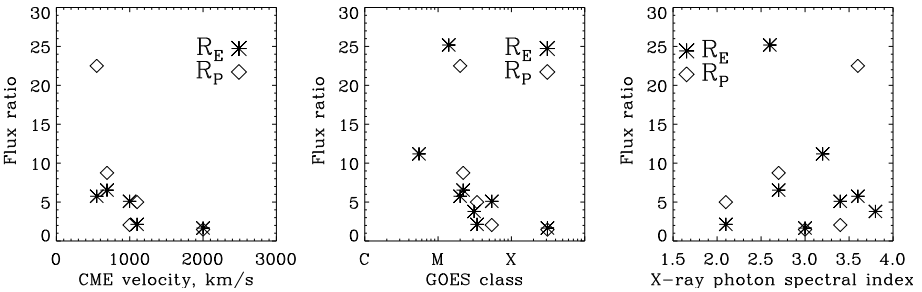

Figure 3 Scatter plots of the electron R_E (marked by *asterisks*) and proton R_P (marked by *diamonds*) flux ratios *vs.* CME projected speed (the *left plot*), *vs.* GOES flare class (*central plot*) and *vs.* X-ray photon spectral index (*right plot*), respectively.

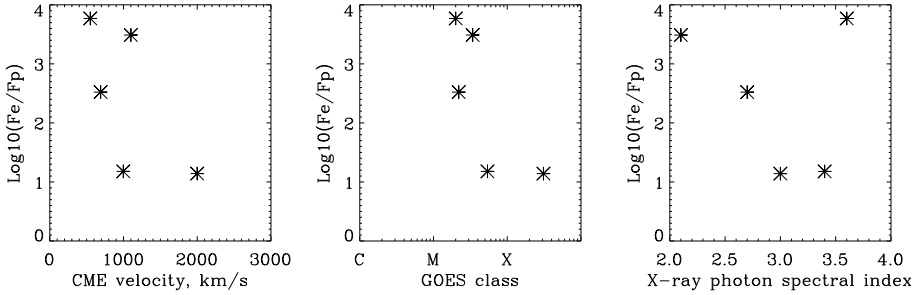

Figure 4 Scatter plots of the logarithm of the electron-to-proton flux ratio *vs.* CME projected speed (*left*), *vs.* GOES flare class (*central plot*), and *vs.* X-ray photon spectral index (*right plot*), respectively.

class, and the X-ray photon spectral index. We obtain a decreasing trend of the particle flux ratios while increasing the CME velocity and GOES flare class. Namely, the highest particle flux ratios occur at the lowest values for CME speed and flare class. This behavior is observed both for protons and electrons. These tendencies could not be fitted by a linear function. The diagram of the particle flux ratios *vs.* the X-ray photon spectral index does not show any tendencies.

Figure 4 presents scatter plots between the electron-to-proton ratio, F_e/F_p, with the CME projected speed, the GOES flare class, and the X-ray photon spectral index, respectively. Since there are only five data points for the analysis (see Table 1, column 7), the statistical significance of the results is low compared with Figure 3. However several tendencies can be noted. The ratio has a tendency to decrease with the CME velocity. This is in a good agreement with the view of a CME as a driver and accelerator of protons in SEP events. One can see a similar tendency for the relation between the abundance ratio and the GOES class flare on the diagram. However, the X-axis of the GOES class flare diagram is logarithmic, while the X-axis in the case of CME velocities is linear. It means that the scattering could only look like a compact dependence. Thus it is more probable that this diagram shows clustering around M3-class flares: the values of the flare class range between M1 and X2. Four out of five points on the scatter plot of the ratio *vs.* the X-ray photon spectral index show a decreasing tendency with softening of the spectral index. The outlier event is accompanied by a relatively slow CME of about 550 km s^{-1}.

4. Discussion

One of the questions we put forward is related to the big flare syndrome. The most powerful flare in the considered set of events (X3.1 on 24 August 2002) produced the most powerful proton event. However, the other X-class flares did not produce any SEP event. We note that the X1 class flare was impulsive with a long decay phase. However, the GOES class of the flares is comparable (X1 and X3.1) and the HXR emission was observed up to the same maximum energy band. The only difference is the CME velocity that differs in about an order of magnitude. The events comparable to the X3.1 flare because of some of the listed parameters (electron-to-proton ratio or electron flux) are associated with M-class flares (M5.4 and M3.4, respectively). In addition, these two flares produced very weak proton fluxes, whereas the other M3.4 class flare produced no particles. The strength of the flare seems not to be a sufficient condition for proton production. Based on these facts we could not claim that the big flare syndrome is evident in the considered active region development.

The left and middle panels of Figure 3 show an increasing tendency of higher energy particles (both 175 – 315 electrons and > 30 MeV protons) to be present with the increase of the CME speed and GOES flare power. Since the slope of either flux ratios cannot be fitted by a straight line, we cannot estimate which trend is stronger; moreover, the horizontal scales are different.

All of the proton-rich SEP events were associated with flares followed by CMEs faster than 500 km s^{-1}. Moreover, there is a tendency of increasing proton fluxes relative to fluxes of electrons with the increase of the CME velocity (Figure 4). In two cases we see that the electron-to-proton ratio is very high (*i.e.* abundance of electrons) in spite of the relatively fast CME velocity. The peculiarity of these two events is the absence of a type II radio burst.

We also investigated if the time delays between HXR, MW, and m-radio emission are indicators of the SEP productive or non-productive flares. The absence of delay between the HXR and MW emission means that the electrons of the same population emit both in MW and HXR and there are no additional wave processes between the accelerated electron precipitation and emission in MW. This parameter could be an indicator if additional processes promote SEP productivity or not. Most SEP productive and proton-rich events had no delay. However, we showed that events 2 and 6 which are related to SEPs had delays of more than 1 s. While both electron and proton enhancements were observed, the events were not proton rich. The X-ray photon spectral indices in these events are harder than 3. This feature could be a result of the lower location of the site of primary energy release in this event relative to the other SEP productive flares. The lower the location the denser the plasma that could prevent direct observations of the MW emission of electrons. The electron-to-proton ratio for both events is high and it could be a result of a stronger magnetic field blocking the escape of the protons to interplanetary space.

For most events, the delays between 40 MHz emission and HXR emission are in good agreement with an average ($0.3c$, with c the velocity of light) or lower velocity of electrons during the type III. For event 3, both the negative delay of radio emission at 150 MHz and 40 MHz relative to HXR and MW emission and the X-ray photon spectral index indicate a high location in the solar corona of the primary energy release. As this event was proton rich, these facts agree with the hypothesis (Daibog, Melnikov, and Stolpovskii, 1993; Daibog *et al.*, 1989) that higher locations of energy release and particle acceleration in the solar atmosphere promote the escape of protons and play the same important role in the generation of proton-rich events as the efficiency of acceleration.

As we noted above the softer HXR spectral index could correspond to a higher location of the acceleration site for similar acceleration processes. We could not find any relation

between the flux ratio in protons or electrons in SEP events with the X-ray photon spectral index of the related solar flare. The electron-to-proton ratio increases with the hardening of the X-ray photon spectral index. This tendency does not coincide with the results by Daibog *et al.* (1989) and Daibog, Melnikov, and Stolpovskii (1993). The reason of this disagreement could be that the authors based their conclusions on impulsive flares. There is only one flare in the studied set of flares which we could identify as a "pure impulsive flare" (event 3). However, this event did not produce an SEP event.

We find that the proton flux increased with the development of the AR. However, there is also no tendency of the X-ray photon index to soften with the AR evolution. Namely, we do not expect the site of the primary energy release to appear in the high corona. A possible explanation for these observations could be sought in the specific topology of the magnetic field. Zhang (2001) proposed two kinds of basic configurations of the magnetic field: the linkage or twist of the lines of force in the ARs. If we have linkage of two flux tubes, we would expect a softening of the HXR spectral index, which is not the case. Thus the magnetic twist model could be an alternative explanation. According to previous studies (Pariat *et al.*, 2017) the evolution of the twisted magnetic flux could result into a stable or unstable configuration. Such an unstable or eruptive configuration is assumed to be very effective for both flare and SEP production. One of the examples is AR10930 observed in December 2006, which presented a clear "vortex"-like structures related to the magnetic topology. However, there is no direct mechanism to affect the spectral index of accelerated particles in this case. In the case of the studied AR we may conclude that the absence of a relationship between the X-ray photon spectral index *vs.* the rising proton-to-electron ratios of the AR could be the result of the development of twisted magnetic fluxes (see Figure 1 in Bogomolov *et al.*, 2014).

All flares of the sample which had emission response in the radio range were followed by type III radio bursts. Four out of nine events did not produce a detectable *in situ* proton flux and none of these were followed by a CME. Namely, the proton abundant SEP events are related with flares followed by CMEs. This strongly supports the hypothesis of proton acceleration due to CME shock waves based on the trends from the current data set.

Summarizing the results of analysis we conclude that:

- The studied data set does not show clear evidence for the big flare syndrome observed during the evolution of the ARs.
- For this set, the high levels of *in situ* protons are always preceded by CMEs.
- There is no indication for a clear relationship between the HXR photon spectral index and SEP properties.
- The delays between HXR and radio emission could point to peculiarities of the acceleration and propagation of energetic particles.

Our results clearly support some of the proposed hypothesis and are opposed to others, similarly to the ambiguous results from statistical studies based on large data sets. A possible reason for the obtained results could be the presence of "vortex"-like features of the magnetic topology of the considered AR. In summary, the magnetic structures and their evolution could be an additional factor determining the SEP productivity of ARs.

Acknowledgements This study is supported by the project 'The origin on solar energetic particles: solar flares *vs.* coronal mass ejections', co-funded by the Russian Foundation for Basic Research with project No. 17-52-18050 and the National Science Fund of Bulgaria under contract No. DNTS/Russia 01/6 (23-Jun-2017). We thank the GOES, ACE, RHESSI and RSTN teams for open access to their data. Authors are thankful to an unknown referee for the detailed reviews and the comments which helped to improve the paper. We thank the team maintaining the CME Catalog at the CDAW Data Center by NASA and the Catholic University of America in cooperation with the Naval Research Laboratory. We are thankful to the SONG team for the data. LKK thanks the budgetary funding of Basic Research program II.16.

Disclosure of Potential Conflicts of Interest The authors claim that they have no conflicts of interest.

Publisher's Note Springer Nature remains neutral with regard to jurisdictional claims in published maps and institutional affiliations.

References

Aschwanden, M.J., Caspi, A., Cohen, C.M.S., Holman, G., Jing, J., Kretzschmar, M., Kontar, E.P., McTiernan, J.M., Mewaldt, R.A., O'Flannagain, A., Richardson, I.G., Ryan, D., Warren, H.P., Xu, Y.: 2017, Global energetics of solar flares. V. Energy closure in flares and coronal mass ejections. *Astrophys. J.* **836**, 17. DOI. ADS.

Bastian, T.S., Benz, A.O., Gary, D.E.: 1998, Radio emission from solar flares. *Annu. Rev. Astron. Astrophys.* **36**, 131. DOI. ADS.

Bogomolov, A.V., Kashapova, L.K., Myagkova, I.N., Tsap, Y.T.: 2014, Dynamics of the hard X-ray, gamma-ray, and microwave emission of solar flares produced by the active region NOAA 0069 in August 2002. *Astron. Rep.* **58**, 156. DOI. ADS.

Bronarska, K., Michalek, G.: 2017, Characteristics of active regions associated to large solar energetic proton events. *Adv. Space Res.* **59**, 384. DOI. ADS.

Cane, H.V., Erickson, W.C., Prestage, N.P.: 2002, Solar flares, type III radio bursts, coronal mass ejections, and energetic particles. *J. Geophys. Res.* **107**, 1315. DOI. ADS.

Cane, H.V., Richardson, I.G., von Rosenvinge, T.T.: 2010, A study of solar energetic particle events of 1997 – 2006: Their composition and associations. *J. Geophys. Res.* **115**, A08101. DOI. ADS.

Daibog, E.I., Melnikov, V.F., Stolpovskii, V.G.: 1993, Solar energetic particle events from solar flares with weak impulsive phases of microwave emission. *Solar Phys.* **144**, 361. DOI. ADS.

Daibog, E.I., Stolpovskii, V.G., Melnikov, V.F., Podstrigach, T.S.: 1989, Microwave bursts and relative concentration of electrons and protons in solar flare cosmic rays. *Pism'a Astron. ž.* **15**, 991. ADS.

Desai, M., Giacalone, J.: 2016, Large gradual solar energetic particle events. *Living Rev. Solar Phys.* **13**, 3. DOI. ADS.

Dierckxsens, M., Tziotziou, K., Dalla, S., Patsou, I., Marsh, M.S., Crosby, N.B., Malandraki, O., Tsiropoula, G.: 2015, Relationship between solar energetic particles and properties of flares and CMEs: Statistical analysis of solar cycle 23 events. *Solar Phys.* **290**, 841. DOI. ADS.

Dulk, G.A.: 1985, Radio emission from the Sun and stars. *Annu. Rev. Astron. Astrophys.* **23**, 169. DOI. ADS.

Fletcher, L., Dennis, B.R., Hudson, H.S., Krucker, S., Phillips, K., Veronig, A., Battaglia, M., Bone, L., Caspi, A., Chen, Q., Gallagher, P., Grigis, P.T., Ji, H., Liu, W., Milligan, R.O., Temmer, M.: 2011, An observational overview of solar flares. *Space Sci. Rev.* **159**, 19. DOI. ADS.

Gopalswamy, N., Yashiro, S., Akiyama, S., Mäkelä, P., Xie, H., Kaiser, M.L., Howard, R.A., Bougeret, J.L.: 2008, Coronal mass ejections, type II radio bursts, and solar energetic particle events in the SOHO era. *Ann. Geophys.* **26**, 3033. DOI. ADS.

Kahler, S.W.: 1982, The role of the big flare syndrome in correlations of solar energetic proton fluxes and associated microwave burst parameters. *J. Geophys. Res.* **87**, 3439. DOI. ADS.

Kennewell, J.A., Cornelius, D.W.: 1983, Learmonth solar observatory. *Ann. UMCS, Sect. AAA Phys.* **20**, 276. ADS.

Kouloumvakos, A., Nindos, A., Valtonen, E., Alissandrakis, C.E., Malandraki, O., Tsitsipis, P., Kontogeorgos, A., Moussas, X., Hillaris, A.: 2015, Properties of solar energetic particle events inferred from their associated radio emission. *Astron. Astrophys.* **580**, A80. DOI. ADS.

Kuznetsov, S.N., Bogomolov, A.V., Galkin, V.I., Denisov, Y.I., Podorolsky, A.N., Ryumin, S.P., Kudela, K., Rojko, J.: 2014, Scientific set of instruments "solar cosmic rays". In: Kuznetsov, V. (ed.) *The Coronas-F Space Mission*, *Astrophys. Space Sci. Lib.* **400**, 289. DOI. ADS.

Lin, R.P.: 2011, Energy release and particle acceleration in flares: Summary and future prospects. *Space Sci. Rev.* **159**, 421. DOI. ADS.

Lin, R.P., Dennis, B.R., Hurford, G.J., Smith, D.M., Zehnder, A., Harvey, P.R., Curtis, D.W., Pankow, D., Turin, P., Bester, M., Csillaghy, A., Lewis, M., Madden, N., van Beek, H.F., Appleby, M., Raudorf, T., McTiernan, J., Ramaty, R., Schmahl, E., Schwartz, R., Krucker, S., Abiad, R., Quinn, T., Berg, P., Hashii, M., Sterling, R., Jackson, R., Pratt, R., Campbell, R.D., Malone, D., Landis, D., Barrington-Leigh, C.P., Slassi-Sennou, S., Cork, C., Clark, D., Amato, D., Orwig, L., Boyle, R., Banks, I.S., Shirey, K., Tolbert, A.K., Zarro, D., Snow, F., Thomsen, K., Henneck, R., McHedlishvili, A., Ming, P., Fivian, M., Jordan, J., Wanner, R., Crubb, J., Preble, J., Matranga, M., Benz, A., Hudson, H., Canfield, R.C., Holman, G.D., Crannell, C., Kosugi, T., Emslie, A.G., Vilmer, N., Brown, J.C., Johns-Krull, C., Aschwanden, M., Metcalf, T., Conway, A.: 2002, The Reuven Ramaty High-Energy Solar Spectroscopic Imager (RHESSI). *Solar Phys.* **210**, 3. DOI. ADS.

McIntosh, P.S.: 1990, The classification of sunspot groups. *Solar Phys.* **125**, 251. DOI. ADS.

Miteva, R., Samwel, S.W., Krupar, V.: 2017, Solar energetic particles and radio burst emission. *J. Space Weather Space Clim.* **7**, A37. DOI. ADS. (15 pp.)

Miteva, R., Klein, K.-L., Malandraki, O., Dorrian, G.: 2013a, Solar energetic particle events in the 23rd solar cycle: Interplanetary magnetic field configuration and statistical relationship with flares and CMEs. *Solar Phys.* **282**, 579. DOI. ADS.

Miteva, R., Klein, K.-L., Samwel, S.W., Nindos, A., Kouloumvakos, A., Reid, H.: 2013b, Radio signatures of solar energetic particles during the 23rd solar cycle. *Cent. Eur. Astrophys. Bull.* **37**, 541. ADS.

Myagkova, I.N., Kuznetsov, S.N., Kurt, V.G., Yuskov, B.Y., Galkin, V.I., Muravieva, E.A., Kudela, K.: 2007, X-ray, γ-emission and energetic particles in near-Earth space as measured by CORONAS-F satellite: From maximum to minimum of the last solar cycle. *Adv. Space Res.* **40**, 1929. DOI. ADS.

O'Flannagain, A.M., Gallagher, P.T., Brown, J.C., Milligan, R.O., Holman, G.D.: 2013, Solar flare X-ray source motion as a response to electron spectral hardening. *Astron. Astrophys.* **555**, A21. DOI.

Onsager, T., Grubb, R., Kunches, J., Matheson, L., Speich, D., Zwickl, R.W., Sauer, H.: 1996, Operational uses of the GOES energetic particle detectors. In: Washwell, E.R. (ed.) GOES-8 *and Beyond*, *Proceedings of the SPIE* **2812**, 281. DOI. ADS.

Papaioannou, A., Sandberg, I., Anastasiadis, A., Kouloumvakos, A., Georgoulis, M.K., Tziotziou, K., Tsiropoula, G., Jiggens, P., Hilgers, A.: 2016, Solar flares, coronal mass ejections and solar energetic particle event characteristics. *J. Space Weather Space Clim.* **6**(27), A42. DOI. ADS.

Pariat, E., Leake, J.E., Valori, G., Linton, M.G., Zuccarello, F.P., Dalmasse, K.: 2017, Relative magnetic helicity as a diagnostic of solar eruptivity. *Astron. Astrophys.* **601**, A125. DOI. ADS.

Reames, D.V.: 1999, Particle acceleration at the Sun and in the heliosphere. *Space Sci. Rev.* **90**, 413. DOI. ADS.

Reames, D.V.: 2015, What are the sources of solar energetic particles? Element abundances and source plasma temperatures. *Space Sci. Rev.* **194**, 303. DOI. ADS.

Reid, H.A.S., Ratcliffe, H.: 2014, A review of solar type III radio bursts. *Res. Astron. Astrophys.* **14**, 773. DOI. ADS.

Salas-Matamoros, C., Klein, K.-L.: 2015, On the statistical relationship between CME speed and soft X-ray flux and fluence of the associated flare. *Solar Phys.* **290**, 1337. DOI. ADS.

Stone, E.C., Frandsen, A.M., Mewaldt, R.A., Christian, E.R., Margolies, D., Ormes, J.F., Snow, F.: 1998, The advanced composition explorer. *Space Sci. Rev.* **86**, 1. DOI. ADS.

Thalmann, J.K., Su, Y., Temmer, M., Veronig, A.M.: 2015, The confined X-class flares of solar active region 2192. *Astrophys. J. Lett.* **801**, L23. DOI. ADS.

Trottet, G., Samwel, S., Klein, K.-L., Dudok de Wit, T., Miteva, R.: 2015, Statistical evidence for contributions of flares and coronal mass ejections to major solar energetic particle events. *Solar Phys.* **290**, 819. DOI. ADS.

White, S.M., Benz, A.O., Christe, S., Fárník, F., Kundu, M.R., Mann, G., Ning, Z., Raulin, J.-P., Silva-Válio, A.V.R., Saint-Hilaire, P., Vilmer, N., Warmuth, A.: 2011, The relationship between solar radio and hard X-ray emission. *Space Sci. Rev.* **159**, 225. DOI. ADS.

Zhang, H.: 2001, Formation of current helicity and emerging magnetic flux in solar active regions. *Mon. Not. Roy. Astron. Soc.* **326**, 57. DOI. ADS.